Fuel retention and carbon deposition on beryllium marker tiles from JET tokamak main chamber limiters investigated by ion beam analysis

P. Tsavalas[a,b] , A. Lagoyannis[a], K. Mergia[a,*], M. Axiotis[a], S. Harissopulos[a], G. Provatas[c], S. Fazinić[c], T. Tadić[c], A. Widdowson[d], M. Rubel[e] and JET Contributors[**]

[a] *National Centre for Scientific Research ''Demokritos'', 15310 Aghia Paraskevi, Athens, Greece*

[b] *National Technical University of Athens, Department of Physics, Zografou Campus, Athens, Greece*

[c] *Ruđer Bošković Institute, Bijenička 54, 10000 Zagreb, Croatia*

[d] *United Kingdom Atomic Energy Authority, Culham Science Centre, Abingdon, OX14 3DB, UK*

[e] *KTH Royal Institute of Technology, Fusion Plasma Physics, 100 44 Stockholm, Sweden*

[**] *See the author list in J. Mailloux et al., Nucl. Fusion* https://doi.org/10.1088/1741-4326/ac47b4

Abstract

JET tokamak with the ITER-like wall is operated with arrays of castellated beryllium limiters in the main chamber. In several locations Be marker tiles were installed for erosion-deposition studies. The castellation sides and the plasma-facing surfaces (PFS) of Be marker tiles from three different locations of the JET main chamber, from the experimental campaigns 2011-12 (ILW-1) and 2013-14 (ILW-2), were analysed employing ^{2}H and ^{3}He micro-beams in order to determine carbon impurity deposition and deuterium retention. The deposited carbon and deuterium amount on the castellation sides (up to 1.5 mm deep into the groove) was assessed with respect to the ion/electron drift direction. Both the carbon and deuterium amount on the investigated castellation sides either stays constant or reduces with depth from the edge of the PFS. No systematic difference is observed in the carbon deposition or deuterium retention on the different castellation sides of each sample with respect to the ion/electron drift direction. Carbon and deuterium content is found to be lower on the PFS than on surfaces in the gaps of castellation for the majority of the samples. The carbon amount is, in general, higher than the deuterium one. No systematic correlation between the carbon and the deuterium amount has been observed.

Keywords: JET tokamak, beryllium, carbon deposition, deuterium retention, ion beam analysis

*Corresponding author: K. Mergia, email: kmergia@ipta.demokritos.gr

1. Introduction

The choice of appropriate plasma-facing materials (PFMs) is an issue of great importance as the plasma-wall interaction (PWI) affects both the lifetime of wall materials and plasma performance. Beryllium (Be) and tungsten (W) are the materials for plasma facing components (PFC) in ITER [1]. Beryllium has been chosen due to its low atomic number which limits plasma dilution and energy radiation losses. This metal has high thermal conductivity (~200 $Wm^{-1}K^{-1}$), low fuel retention in comparison to carbon (C) which reacts chemically with H isotopes [2] and it is an efficient oxygen getter thus reducing oxygen impurities and helps to keep the effective atomic number, Z_{eff}, in the vessel at low levels. A detailed overview of beryllium as PFC is presented in [3].

Until 2009 the Joint European Torus (JET) at the Culham Science Centre, the largest tokamak in the world, was operated with carbon as the main PFM (JET-C) [4]. Very high fuel inventories were measured because the presence of carbon is decisive for fuel retention by co-deposition [5]. This called for a large-scale test of a metal wall. Since 2011 JET has metallic PFC, called the ITER-like wall (JET-ILW) [6]. Beryllium is in the main chamber (castellated limiters and Be coatings on the inner wall cladding) and tungsten in the divertor: the load bearing plate in the base made of bulk metal, while W-coated carbon fiber composites tiles are in other locations. Three experimental campaigns were performed in 2011-2016 with deuterium fuelling: 2011-12 (ILW-1), 2013-14 (ILW-2) and 2015-16 (ILW-3) with input energy of 150, 201 and 245 GJ, respectively. The overview has been presented in [7], while detailed works have dealt with erosion, material deposition and deuterium (D) retention on the surface of the divertor [8, 9, 10, 11, 12, 13, 14, 15, 16, 17, 18] and on the main chamber [19, 20, 21, 22, 23, 24, 25, 26]. In addition, material deposition and fuel retention on surfaces located in the gaps of the castellated Be limiters have been examined [27, 28, 29]. It has also been consistently shown that fuel inventory with ILW was reduced by one order of magnitude in comparison to JET-C [30, 31]. The main source of carbon in JET was eliminated, but still the knowledge of the carbon content in co-deposits and the carbon-deuterium correlation is crucial for the detailed assessment of factors influencing the retention in JET-ILW and, by this, for improved predictions for ITER. Two are the sources of carbon after the JET transformation to a fully metallic device, a) the carbon residuals from the previous wall and b) the carbon fiber composite (CFC) tiles coated by tungsten in the divertor [32].

The relation between the co-deposition and the deuterium retention in JET-ILW had been investigated in detail on W-coated divertor tiles. Works [10, 12, 14, 24] report that the retention increases with the increase of the material (Be and C) deposition. The works [13, 15, 16, 17] claim that the increase of the D retention is due to Be deposition, while [8, 18] report that the C deposition increases the D retention. The C-D correlation in Be has also been investigated, on laboratory-prepared samples. Anderl et al. found the retention in pure Be to be lower than in C-coated beryllium [33]. Also Guseva et al [34] concluded that carbon impurities on the Be surface enhance the D retention. On the other hand, C. Porosnicu et al. irradiated different beryllium-carbon relative concentration with deuterium ions and found that lower carbon concentration retained higher deuterium content [35]. Thus, it is not clear from the literature whether the residual deuterium retention still exists as a result of the C-D chemistry or whether D is integrated into deposits irrespective of C.

Accelerator-based ion beam analysis (IBA) is the most efficient set of methods in surface studies of wall materials [36]. Among them, a ^{3}He-based nuclear reaction analysis (NRA) has

been the most frequently used for the simultaneous determination of D, Be, C in carbon-wall machines. In the case of JET-ILW, the C quantification on Be surfaces is not possible with the $^{12}C(^{3}He,p_0)^{14}N$ reaction due to its superposition with the $^{9}Be(^{3}He,p_3)^{11}B$ one, as detailed in [36]. The remaining options are in: (i) proton scattering via $^{12}C(p,p)^{12}C$ [37, 38] with the sensitivity at the level of $1x10^{17}$ ^{12}C cm^{-2}, (ii) heavy ion elastic recoil detection analysis (HIERDA) with high sensitivity (below $1x10^{15}$ ^{12}C cm^{-2}) but the information depth limited to less than 1 μm, (iii) NRA using a ^{2}H beam via $^{12}C(^{2}H,p)^{13}C$. The latter method (with sensitivity of $1x10^{15}$ ^{12}C cm^{-2}) was applied for carbon studies in this paper.

A study of the carbon deposition on plasma-facing surfaces (PFS) and inside the castellation grooves of JET-ILW limiters was performed earlier with a standard ^{2}H milli-beam [29]. In the current work we investigate whether carbon deposition on the castellation sides is affected by the orientation of the castellation side with respect to the ion or electron drift direction. Moreover, a ^{2}H micro-beam has been applied to examine the morphology of carbon deposition. Deuterium retention is investigated by the use of a ^{3}He micro-beam on both the PFS and the castellation sides. Whether carbon or deuterium are co-deposited with beryllium or not cannot be verified with the present study. The overall aim is to quantify carbon and deuterium on the castellation and plasma-facing surfaces of the JET-ILW beryllium marker tiles and investigate if carbon plays a role in the retention of deuterium in the deposits.

2. Materials and Experimental Details

Samples from different marker tiles of the main chamber and after the first and the second experimental campaigns were investigated: one sample from the upper Dump Plate (DP, 2B(C)2), two from the mid-plane of Outer Poloidal Limiter (OPL, 4D14) and four from the Inner Wall Guard Limiter (IWGL, 2XR10) (Figure 1). These tiles are castellated in order to reduce the eddy currents and thermal stresses [39], and therefore, the castellation sides are free to interact with the plasma. Moreover, the samples from the marker tiles have a nickel interlayer between the top beryllium layer and the bulk beryllium [40]. After the cut, one of the castellation sides was marked for reference reasons. The configuration of the tiles and the samples as well as the labelling of the castellation sides based on the ion/electron drift direction of ILW1 IWGL outer (27) sample, as an example, are presented schematically in Figure 2.

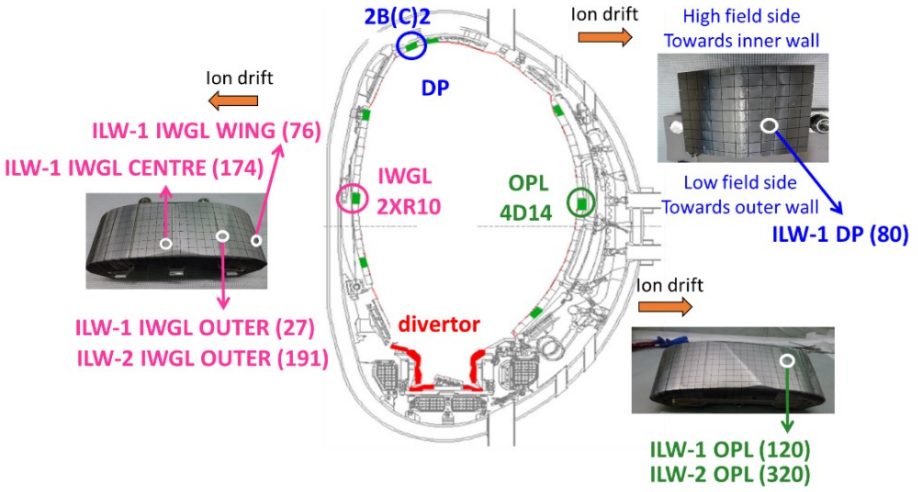

Figure 1: Position of the investigated Tiles and samples inside the main chamber of the JET tokamak.

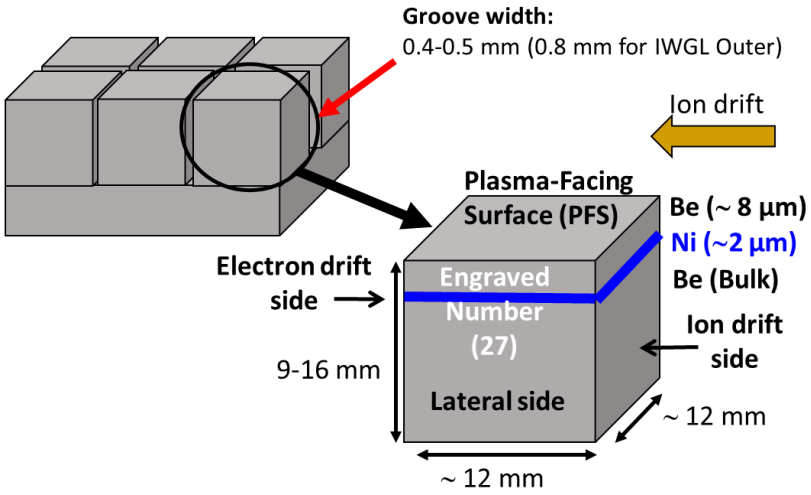

Figure 2: Schematic of the castellation configuration of the beryllium tiles and the configuration of the ILW1 IWGL outer (27) sample. The castellation sides are labelled based on the ion/electron drift direction.

The ^{2}H micro- and milli- beam measurements were performed using the 5.5 MV TN11 HV Tandem Accelerator at NCSR "Demokritos", in Athens, Greece. The beam energy was 1.35 MeV and a silicon surface barrier (SSB) detector with depletion depth of 1000 µm was placed at an angle of 170^{o} with respect to the beam axis. A kapton foil of 12.5 µm was positioned in front of the detector in order to separate the peak $^{12}C(d,p_0)^{13}C$ used for the carbon quantification from the peaks of alpha particles emitted via $^{9}Be(d,a_0)^{7}Li$ and $^{9}Be(d,a_1)^{7}Li$ reactions. The chamber was kept under vacuum (10^{-6} mbar). The beam spot of the micro-beam had a diameter smaller than 100 µm and the current was around 100 pA. The mapping

area was 1.5 x 1.5 mm^2 and the resolution 64 x 64 pixels. The data acquisition and the mapping was performed using the OMDAQ2007 software and appropriate hardware [41].

The ^{3}He measurements were carried out at Ruder Boskovic Institute, in Zagreb, Croatia. The ^{3}He beam was accelerated by the 6 MV tandem Van de Graaff accelerator and 1.0 MV Tandetron accelerator. The beam energies varied between 2 and 3 MeV, and the mapping areas were either 1 × 1 mm^2 or 300 × 300 μm^2. A Partially Depleted Silicon Surface Barrier detector (PDSSB) with depletion depth of 2000 μm, with nominal active area of 300 mm^2 collimated to 230 mm^2 was used and placed at an angle of 135^o ± 19^o with respect to the beam axis. The distance between the target and the detector was approximately 2.5 cm, which corresponds to a solid angle of 0.462 sr. Additionally, a Mylar foil of 120 μm thickness was placed before the detector in order to absorb the alpha particles produced via ^{9}Be(^{3}He,a)^{8}Be reactions and to detect only the ^{9}Be(^{3}He,p)^{11}B and ^{2}H(^{3}He,p_0)^{3}He peaks. A chopper was used in order to estimate the collection charge of the measurements. The data acquisition of the ^{3}He beam was performed using the in-house developed software package SPECTOR [42] and the hardware based on Xilinx Virtex 6 FPGAs; for more technical details see [43].

It is noted that the investigated area from the castellation sides is at the entrance of the gap, ranging from 0.3 to 1.5 mm into the gap, since according to M. Rubel et al. [28] the majority of the deuterium retention is restricted in this area.

The quantitative analysis of all the NRA spectra was performed with the SIMNRA software [44]. For the ^{3}He micro-beam NRA measurements and the deuterium quantification, the V. Kh. Alimov et al [45] cross section data for the ^{2}H(^{3}He,p_0)^{4}He reaction and the N. P. Barradas et al [46] one for the ^{9}Be(^{3}He,$p_{0,1}$)^{11}B reactions were used. For the ^{2}H beam NRA measurements and the carbon quantification, the evaluated cross section data from SigmaCalc archive [47] and P. Tsavalas et al [48] for the ^{12}C(^{2}H,p_0)^{13}C and ^{9}Be(^{2}H,p_0)^{10}Be reactions, respectively, were used.

3. Results and discussion

3.1 Carbon deposition

The carbon content was measured on ion and/or electron drift sides, as well as on some lateral castellation sides, employing a ^{2}H beam. Figure 3 presents a representative NRA spectrum together with the simulated spectrum from the lateral side of the sample 27 (ILW1 IWGL outer) using ^{2}H micro-beam. In this figure, the energy range with the peaks corresponding to the nuclear reactions ^{12}C(^{2}H,p_0)^{13}C and ^{9}Be(^{2}H,p_0)^{10}Be is shown. The quantitative results of the determined carbon and deuterium amounts from a) the PFS and b) the castellation sides up to a maximum depth of 1.5 mm from the edge of the PFS are presented in Figure 4. The absence of C or D content for some castellation sides (C content on the ion drift side of ILW1 IWGL outer (27) and D content on the ion drift side ILW2 OPL (320), the electron drift side of ILW1 DP (80), and the lateral sides of ILW1 IWGL outer (27), ILW2 IWGL outer (191) and ILW1 centre (174)) is due to the lack of experimental data. The deposited carbon amount on the PFS is from our previous study [29]. It is observed that the orientation of the castellation side does not, in general, affect significantly carbon deposition. Only for sample 27 from the ILW1 IWGL outer, almost one order of magnitude higher carbon amount ((59±4) × 10^{17} at/cm^2) is found for the lateral side compared to the

electron drift one. On all the other castellation sides carbon deposition ranges from (3.2±0.2) × 10^{17} at/cm^2 to (19±1) × 10^{17} at/cm^2, with the ILW1 Dump Plate (80) presenting systematically the higher carbon deposition on its castellation sides and the IWGL 2XR10 Centre (174) the lowest. A trend of higher carbon amount on the castellation sides than that on the PFS is observed.

In Figure 5 the carbon mapping of the lateral side of all samples is depicted, with the exception of the ILW1 IWGL centre (174) sample, for which the ion drift side is presented. The PFS of the samples is at the top of the mapping and it is defined by a white line. On the ILW1 DP (80), some carbon agglomerates with diameter of about 150 µm have been formed over the whole side. On the ILW1 OPL (120), we observe a slight decrease of carbon with the depth. On the ILW2 OPL (320), carbon agglomerates with diameter in the range 100 – 200 µm are observed near the PFS of the sample. On ILW1 IWGL outer (27), at a depth of about 800 µm from the PFS, a stripe rich in carbon, having a width of about 500 µm, has been formed. On ILW2 IWGL outer (191), the amount of carbon decreases as a function of depth. On the ILW1 IWGL centre (174), 400 µm from the PFS, there is a thin stripe, having a width of about 200 µm, depleted of carbon. On the IWL1 IWGL wing (76), a drastic decrease of the carbon content with depth is observed.

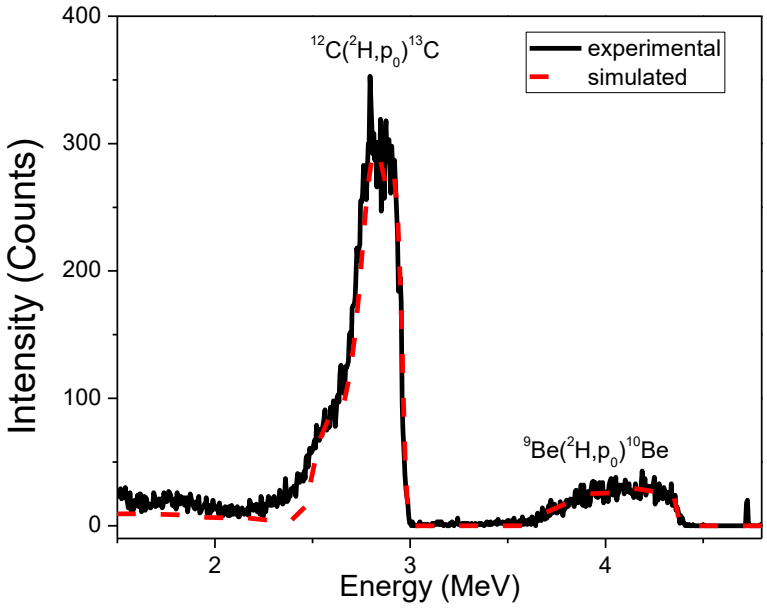

Figure 3: The measured (solid black line) and simulation (dash red line) NRA spectrum of ILW-1 IWGL Outer (27) castellation side using a ^{2}H micro-beam.

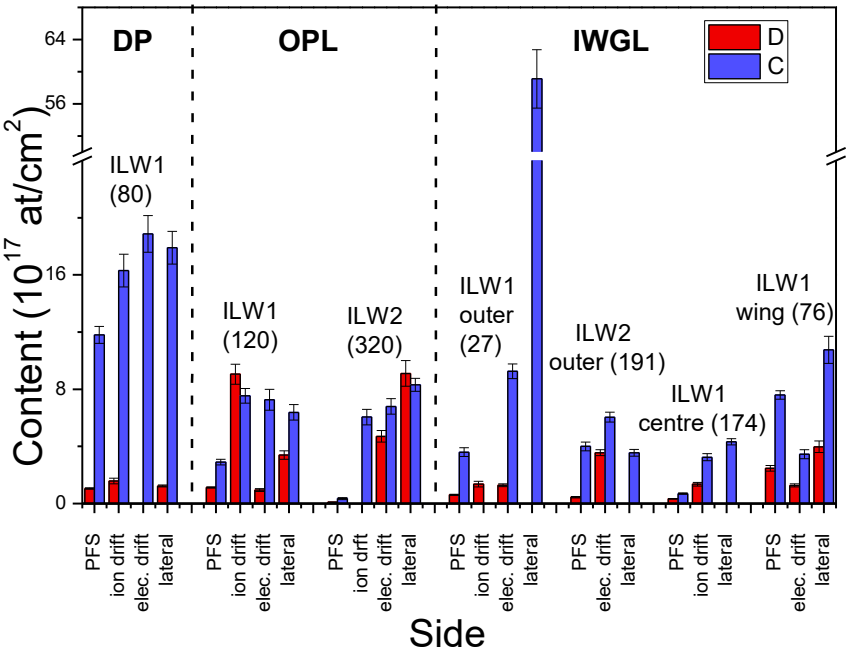

Figure 4: Deuterium and carbon content of the plasma-facing surface (PFS) and the castellation sides as measured by ^{3}He and ^{2}H beams, respectively.

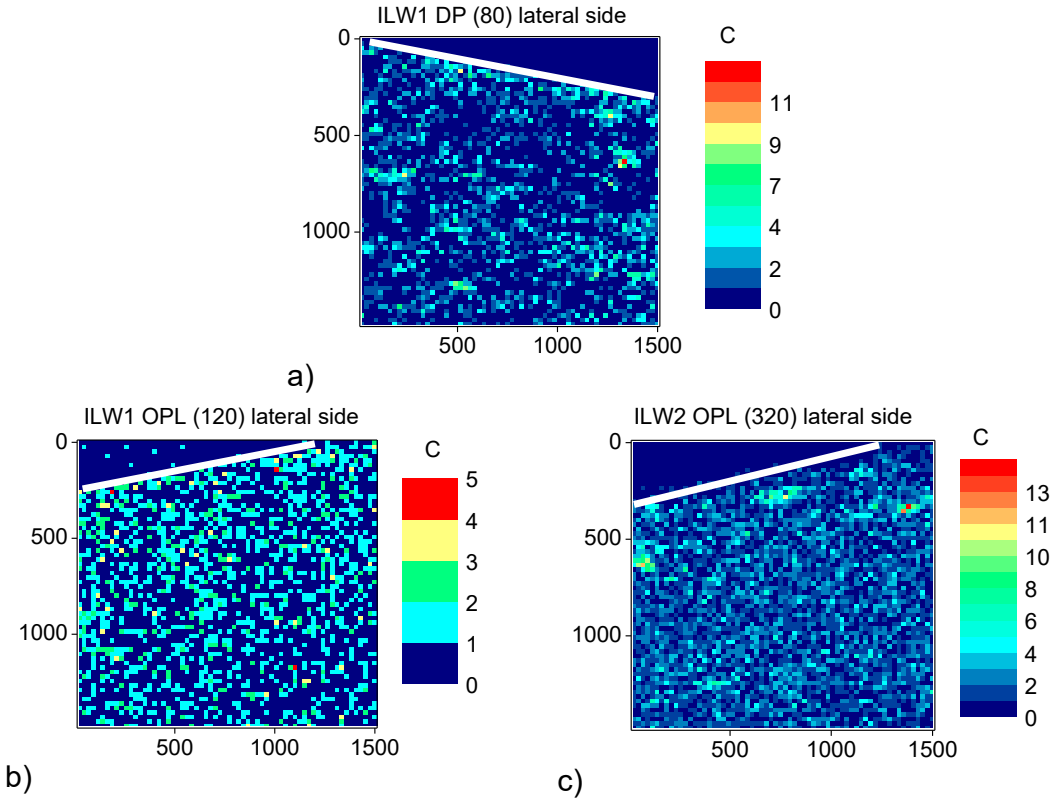

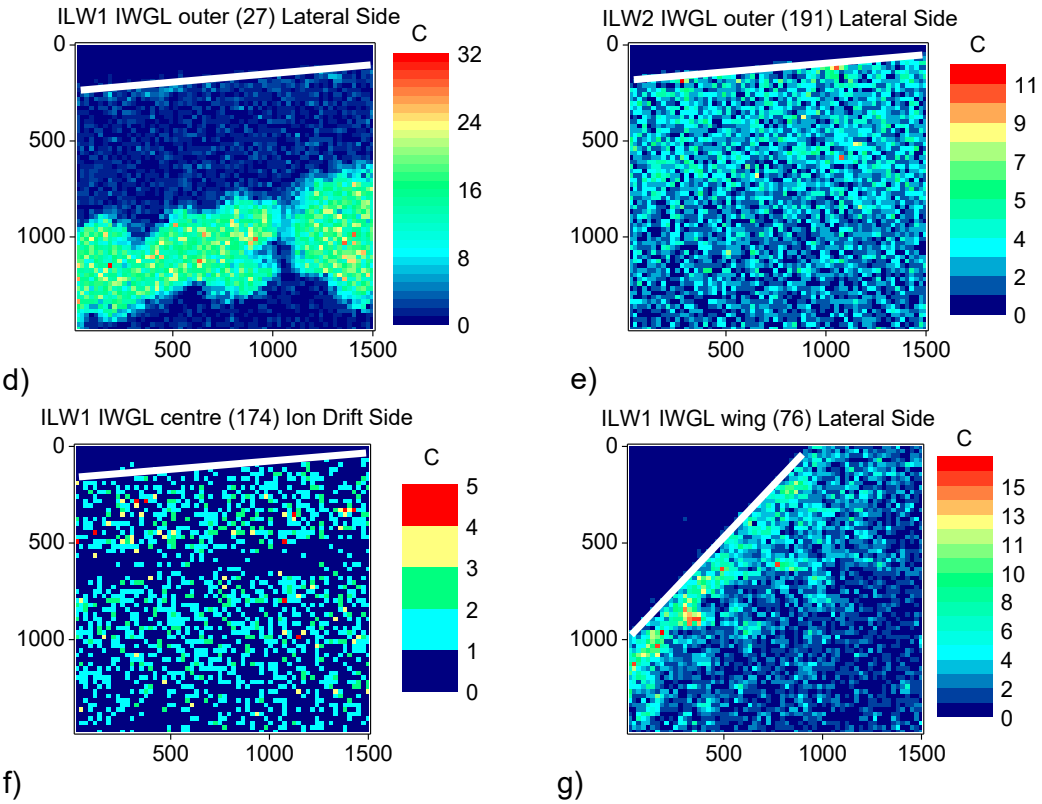

Figure 5: Mapping of the deposited carbon on the lateral side (a, b, c, d, e, g) and the ion drift side of the ILW1 IWGL centre (174) (f). The white line defines the edge of the plasma-facing surface. The unit of the axes is µm.

3.2 Deuterium retention

The PFS and at least one castellation side of all the samples were measured using a ^{3}He micro-beam. Figure 6 depicts representative experimental and simulated spectra of the ion drift side from the ILW1 Dump Plate (80) employing a ^{3}He micro-beam. The determined deuterium content using a ^{3}He beam is presented in Figure 4.

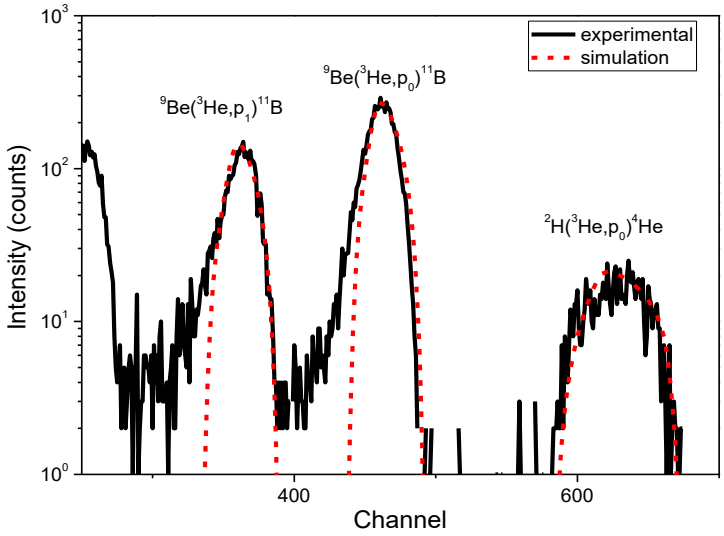

Figure 6: The experimental (black solid line) and the simulated (red dashed line) NRA spectra of the ion drift side of sample 80 from the ILW1 Dump Plate.

The deuterium content on the PFS of the samples is found to vary more than one order of magnitude, ranging from (0.090±0.003) × 10^{17} at/cm^2 (sample 320 from ILW2 OPL) to (2.5±0.2) × 10^{17} at/cm^2 (sample 76 from IWGL 2XR10 wing). The deuterium amount determined in the current work on the PFS of ILW1 DP ((1.05±0.05) × 10^{17} at/cm^2) is in reasonable agreement with that reported in [24] ((3.4±1.2) × 10^{17} at/cm^2). Additionally, integrating the mean D content (1.2×10^{17} at cm^{-2}) of the different areas over the whole ILW1 IWGL tile, we observe that the total D content, 3.51×10^{19} at, is half of the corresponding value (6.76×10^{19} at) reported in [24].

On the castellation sides, the variation of the fuel retention between the various locations is reduced with the deuterium content ranging between (0.96±0.10) × 10^{17} at/cm^2 (ILW1 OPL (120) electron drift side) and (9.1±0.9) × 10^{17} at/cm^2 (ILW1 OPL (120) ion drift side and ILW2 OPL (320) lateral side). In general the castellation sides retain higher amounts of deuterium than the PFS.

From the first to the second campaign, the deuterium content on the PFS decreased; for the OPL from (1.13±0.04) x 10^{17} at/cm^2 to (0.090±0.003) × 10^{17} at/cm^2 and for IWGL outer from (0.61±0.04) × 10^{17} at/cm^2 to (0.45±0.05) × 10^{17} at/cm^2. On the contrary, deuterium amount on the castellation sides during ILW2 increases with respect to ILW1; for OPL from (0.95±0.10) × 10^{17} at/cm^2 to (4.7±0.4) × 10^{17} at/cm^2 (electron drift side) and from (3.4±0.3) x 10^{17} at/cm^2 to (9.1±0.9) x 10^{17} at/cm^2 (lateral side); and for IWGL outer from (1.4±0.2) x 10^{17} at/cm^2 to (3.8±0.2) x 10^{17} at/cm^2 (electron drift side).

Subsequently, the mean values of the deuterium content on the castellation sides are compared with those reported in [25]. There is agreement that the ILW1 DP castellation sides present the lowest deuterium retention with (1.4±0.3) × 10^{17} at/cm^2 found in the current work and <10^{17} at/cm^2 reported in [25]. For the ILW1 OPL castellation side, the value found in the current work ((4.5±2.4) × 10^{17} at/cm^2) is very close with that reported in [25] (~6×10^{17} at/cm^2). For the ILW1 IWGL, we find lower deuterium amount ((1.8±0.5) × 10^{17} at/cm^2) than the low limit of the range reported in [25] ((7-20) × 10^{17} at/cm^2).

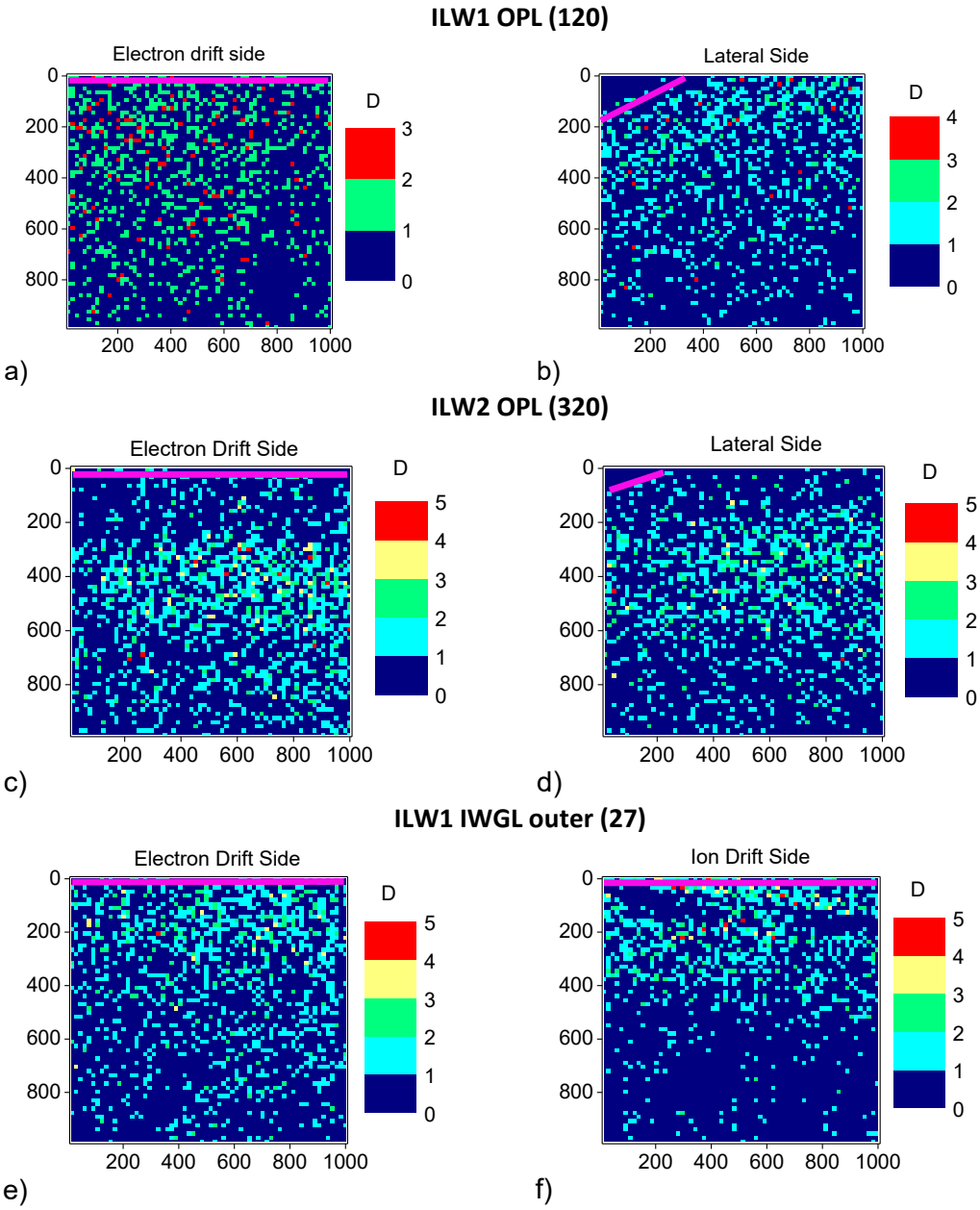

Figure 7: Deuterium mapping of castellation sides. The top magenta line defines the edge of the plasma-facing surface. The unit of the axes is µm.

Figure 7 depicts deuterium mappings of some of the castellation sides for IWL1 OPL (120), ILW2 OPL (320) and ILW1 IWGL outer (27), as determined with the ^{3}He micro-beam. The deuterium distribution on the PFS is homogeneous for all samples and therefore deuterium mappings of the PFS are not presented. On the other hand, deuterium is reduced with depth on the castellation sides of all samples apart from the ILW2 OPL (320) (Figure 7c and d) where a deuterium stripe of about 400 µm width, 200 µm from the PFS edge, is observed for both castellation sides. The deuterium distribution is similar on the castellation sides of ILW1 OPL (120) (Figure 7a and b). On the ion drift side of the IWL1 IWGL outer (27) (Figure 7f) the deuterium is reduced with depth more abruptly than on electron drift one (Figure 7e).

3.3 Deuterium retention versus carbon deposition

In this section we discuss possible correlation between deuterium retention and carbon deposition. From Figure 4, we conclude that high carbon amount is not necessarily accompanied by high deuterium content.

In Figure 8 the deuterium over carbon ratio (D/C) is presented for the PFS and the castellation sides. For the castellation sides the average content of C and D has been used. The D/C ratio ranges from 0.08 to 1.17 with DP presenting the smallest ratio (<0.1) and the castellation sides of OPL after the second campaign the highest one (~1). Similar D/C ratios for the PFS and the castellation sides are observed during ILW1 campaign, whereas during ILW2 campaign the ratio is larger on the castellation sides compared to that of the PFS, being in the range of 3.8 - 6.6.

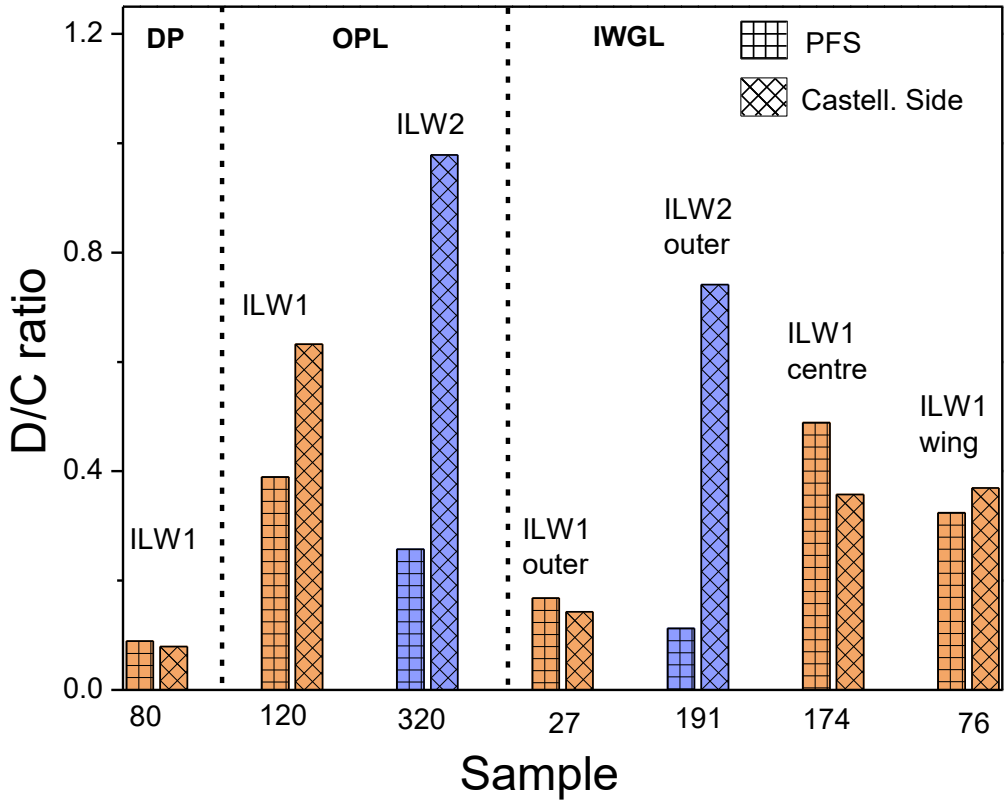

Figure 8: The deuterium over carbon (D/C) ratio of the plasma-facing surface (PFS) and the castellation. For the castellation the average of the measured castellation sides has been used.

Next we discuss the carbon and deuterium mappings from the same castellation side. Figure 9 depicts representative carbon and deuterium mappings of three castellation sides. The white line defines the edge of the plasma-facing surface. In Figure 9j the edge of the castellation side is not well defined, because the castellation side was not perfectly aligned with respect to the ion beam so signal from the PFS was also detected.

ILW1 DP (80) Lateral Side

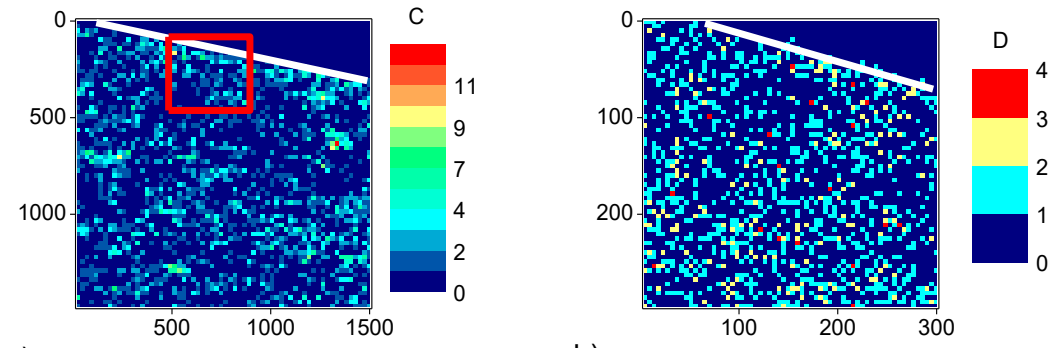

a) b)

ILW1 OPL (120) Lateral Side

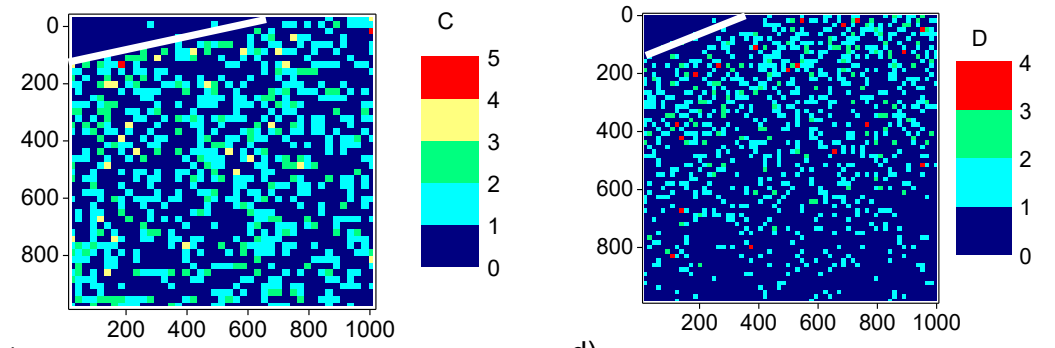

c) d)

ILW2 OPL (320) Lateral Side

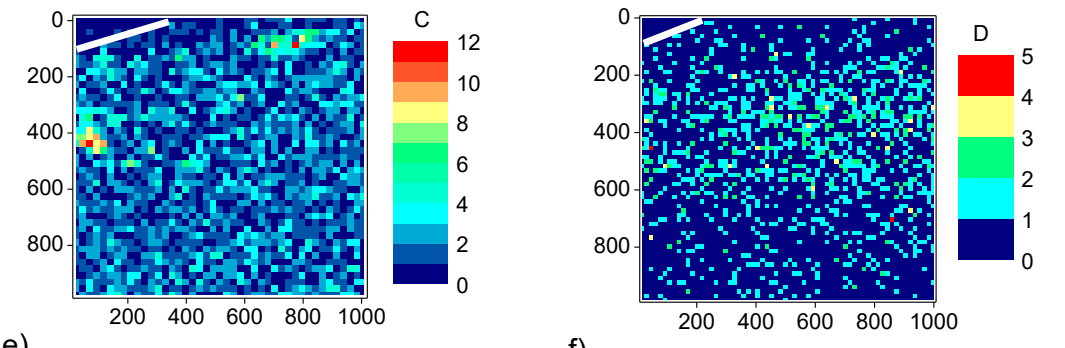

e) f)

ILW1 IWGL centre (174) Ion Drift Side

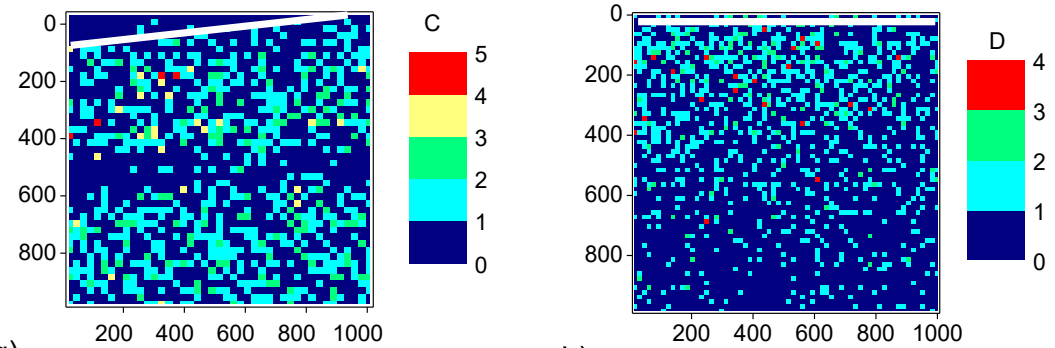

g) h)

ILW1 IWGL wing (76) Lateral Side

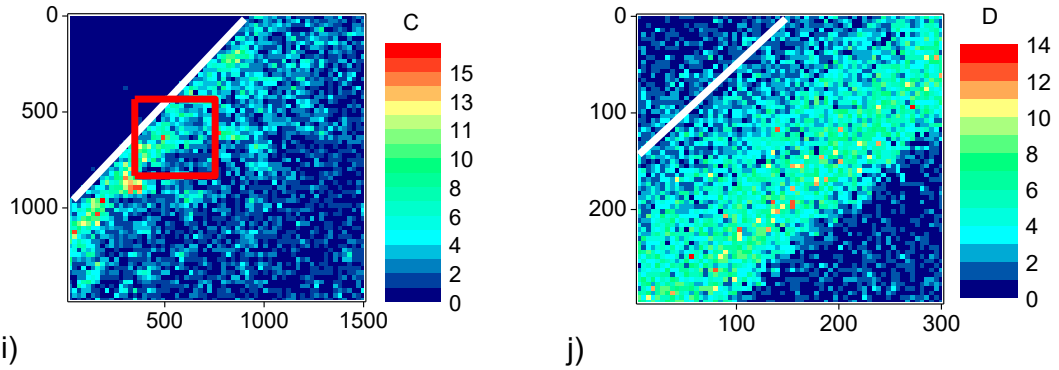

Figure 9: Carbon and deuterium mapping of the same castellation side of ILW1 DP (80) (a and b), ILW1 OPL (120) (c and d), ILW2 OPL (320) (e and f), ILW1 IWGL centre (174) (g and h) and ILW1 IWGL wing (76) (i and j). The area of deuterium mapping for b) and f) corresponds to the red square of the corresponding carbon mapping. The white line defines the edge of the plasma-facing surface. The unit of the axes is µm.

On ILW1 DP (80) lateral side (Figure 9a and b), carbon and deuterium have similar homogeneous distributions all over the mapped area. On the ILW1 OPL (120) lateral side the carbon distribution is nearly homogeneous (Figure 9c) while the deuterium decreases with depth (Figure 9d). On the ILW2 OPL (320) lateral side the stripe rich in deuterium (Figure 9f) is not observed on the carbon mapping (Figure 9e). On the ILW1 IWGL centre (174) ion drift side, there is a zone depleted of carbon (Figure 9g), while the amount of deuterium decreases smoothly with depth (Figure 9h). On ILW1 IWGL wing (76) lateral side, a similar stripe with high amount of carbon and deuterium is detected near the PFS (Figure 9i and j).

4. Summary and Conclusions

The PFS and castellation sides of samples from different beryllium marker tiles of the main chamber and after different campaigns of the JET tokamak were investigated employing ion beam analysis using ^{2}H and ^{3}He beams in order to assess carbon deposition and deuterium retention, respectively, their spatial distribution, their content with respect to the ion/electron drift direction and the correlation between them.

The carbon maps show that, in general, the carbon amount on the investigated castellation sides either stays constant or reduces with depth from the edge of the PFS. No systematic difference is observed in the carbon deposition on the different castellation sides of each sample with respect to the ion/electron drift direction.

Concerning deuterium, the PFS of the majority of the samples has retained less amount than that retained on the castellation sides. From the first to the second campaign the deuterium amount of the PFS decreases, while on the castellation sides it increases. The deuterium distribution on the PFS is homogeneous while on the castellation sides it decreases with depth for the large majority of the samples. Additionally, the carbon amount is, in general, higher than the deuterium one. No systematic correlation between the carbon and the deuterium amount has been observed.

Acknowledgments

This work has been carried out within the framework of the EUROfusion Consortium, funded by the European Union via the Euratom Research and Training Programme (Grant Agreement Nos 633053 and 101052200 - EUROfusion). Views and opinions expressed are however those of the author(s) only and do not necessarily reflect those of the European Union or the European Commission. Neither the European Union nor the European Commission can be held responsible for them. The funding from the General Secretariat for Research and Innovation of the Greek National Programme of the Controlled Thermonuclear Fusion is acknowledged. Furthermore, this project was supported by "CALIBRA/EYIE" (MIS 5002799) which is implemented under the Action "Reinforcement of the Research and Innovation Infrastructure", funded by the Operational Program "Competitiveness, Entrepreneurship and Innovation" (NSRF 2014-2020) and co-financed by Greece and the European Union (European Regional Development Fund).

1 References

[1] V. Barabash, G. Federici, R. Matera, A. R. Raffray, and ITER Home Teams, *Armour Material for the ITER Plasma Facing Components*, Phys. Scr. 1999, T81, 1999, 74-83 https://doi.org/10.1238/Physica.Topical.081a00074

[2] S. Brezinsek, T. Loarer, V. Phillips, H. G. Esser, S. Grunhagen, R. Smith, R. Felton, J. Banks, P. Belo, A. Boboc, J. Bucalossi, M. Clever, J.W. Coenen, I. Coffey, D, Douai, M. Freisenger, D. Frigione, M. Groth, A. Huber, J. Hobirk, S. Jachmich, S. Knipe, U. Kruezi, G.F. Mathews, A.G. Meigs, F. Nave, I. Nunes, R. Neu, J. Roth, M.F. Stamp, S. Vartagnian, U. Samm and JET EFDA contributors, *Fuel retention studies with ITER-Like Wall in JET*, Nucl. Fusion 53, 2013, 083023 (13pp) https://doi.org/10.1088/0029-5515/53/8/083023

[3] G. De Temmerman, K. Heinola, D. Borodin, S. Brezinsek, R. Doerner, M. Rubel, E. Fortuna-zalesna, C. Linsmeier, D. Nishijima, k. Nordlund, M. Robst, J. Romazanov, E. Safi, T. Schwarz-Selinger, A. Widdowson, B. J. Braams, H-K Chung, C. Hill, *Data on erosion and hydrogen fuel retention in Beryllium plasma-facing materials*, Nucl. Mater. Energy 27, 2021, 100994 https://doi.org/10.1016/j.nme.2021.100994

[4] J.P. Coad, M. Rubel, J. Likonen, N. Bekris, S. Brezinsek, G. F. Matthews, M. Mayer, A.M. Widdowson, JET contributors, *Material migration and fuel retention studies during the JET carbon divertor campaigns,* Fusion Eng. Des 138, 2019, 78 https://doi.org/10.1016/j.fusengdes.2018.10.002

[5] J. Roth, E. Tsitrone, A. Loarer , G. Counsell, R. Neu, V. Philipps, S. Brezinsek, M. Lehnen, P. Coad, Ch. Grisolia, K. Schmid, K. Krieger, A. Kallenback, B. Lipschultz, R. Doerner, R. Causey, V. Alimov, W. Shu, O. Ogorodnikova, A/ Kirschner, G. Federici, A. Kukunshkin, EFDA PWI Task Force, ITER PWI Team, Fusion for Energy, ITPA SOL/DIV, *Recent analysis of key plasma wall interactions issues for ITER*, J. Nucl. Mater. 390-391, 2009, 1-9 https://doi.org/10.1016/j.jnucmat.2009.01.037

[6] G.F. Matthews, P. Edwards, T. Hirai, M. Kear, A. Lioure, P. Lomas, A. Loving, C. Lungu, H. Maier, P. Mertens, D. Neilson, R. Neu, J. Pamela, V. Philipps, G. Piazza, V. *Overview of ITER-like Wall Project*, Phys. Scr. T128, 2007, 137 https://doi.org/10.1088/0031-8949/2007/T128/027

[7] X. Litaudon et al, *Overview of the JET results in support to ITER*, Nucl. Fusion 57, 2017, 102001 https://doi.org/10.1088/1741-4326/aa5e28

[8] J. P. Coad, E. Alves, N. P. Barradas, A. Baron-Weichec, N. Catarino, K. Heinola, J. Likonen, M. Mayer, G. F. Mathews, P. Petersson, .A. Widdowson and JET-EFDA Contributors, *Surface analysis of the tiles and samples exposed the first JET campaigns with the ITER-like wall,* Phys. Scr T159, 2014, 014012 (5pp) https://doi.org/10.1088/0031-8949/2014/T159/014012

[9] P. Petersson, M. Rubel, H. G. Esser, J. Likonen, S. Koivuranta, A. Widdowson and JET-EFDA Contributors, *Co-deposited layers in the divertor region of JET-ILW*, J. Nucl. Mater. 463, 2015, p. 814-817 https://doi.org/10.1016/j.jnucmat.2014.12.077

[10] M. Mayer, S. Krat, W. Van Renterghem, A. Baron-Weichec, S. Bresinsek, I. Bykov, P. Coad, Yu Gasparyan, K. Heinola, J. Likonen, A. Pisarev, C. Ruset, G. de Saint-Aubin, A. Widdowson and JET Contributors, *Erosion and deposition in the JET divertor during the first ILW campaign*, Phys. Scr. T167, 2016, 0144051 (9pp) https://doi.org/10.1016/j.jnucmat.2014.12.077

[11] A. Lagoyannis, P. Tsavalas, K. Mergia, G. Provatas, K. Triantou, E Tsompopoulou, M. Rubel, P. Petersson, A. Widdowson, S Harissopulos, T. J. Mertzimekis and the JET contributors, *Surface composition and structure of divertor tiles following the JET tokamak operation with the ITER-like wall*, Nucl. Fusion 57, 2017, 076027 (7pp) https://doi.org/10.1088/1741-4326/aa6ec1

[12] N. Catarino, N.P. Barradas, V. Corregidor, A. Widdowson, A. Baron-Weichec, J.P. Coad, K. Heinola, M. Rubel, E. Alves, JET Contributors, *Assessment of erosion, deposition and fuel retention in the JET-ILW divertor from ion beam analysis data*, Nucl. Mater. Energy 12, 2017, 559-563 https://doi.org/10.1016/j.nme.2016.10.027
[13] Y. Zhou, H. Bergsaker, I, Bykov, P. Petersson, G. Possnert, J. Likonen, J. Pettersson, S. Koivuranta, A.M. Wddowson, JET contributors, *Microanalysis of deposited layers in the inner divertor of JET with ITER-like wall, Nucl. Mater. Energy* 12, 2017, 412-417 https://doi.org/10.1016/j.nme.2017.02.015
[14] J. Likonen, K. Heinola, A. De Backer, A. Baton-Wiechec, N. Catarino, I. Jepu, C.F. Ayres, P. Coad, G.F. Matthews, A. Widdowson, JET Contributors, *Investigation of deuterium trapping and release in the JET divertor during the third ILW campaign using TDS*, Nucl. Mater. Energy 19, 2019, p. 300 - 306 https://doi.org/10.1016/j.nme.2019.03.012
[15] P. Strom, P. Petersson, M. Rubel, E. Fortuna-Zalesna, A. Widdowson, G Sergienko, JET Contributors, *Analysis of deposited layers with deuterium and impurity elements on samples from the divertor of JET ITER-like wall,* J. Nucl. Mater. 516, 2019, 202-213 https://doi.org/10.1016/j.jnucmat.2018.11.027
[16] N. Catarino, A. Widdowson, A. Baron-Wiechec, J.P. Coad, K. Heinola, M. Rubel, N.P. Barradas, E. Alves and JET Contributors, *Deposition in the tungsten divertor during the 2011-2016 campaigns in JET with ITER-like wall*, Phys. Scr., T171, 2020, 014044 (7pp) https://doi.org/10.1088/1402-4896/ab4df7
[17] S. Krat, M. Mayer, A. Baron-Wiechec, S. Brezinsek, P. Coad, Yu Gasperyan, K. Heinola, I. Jepu, J. Likonen, P. PEtersson, C. Ruset, G. de Saint-Aubin, A. Widdowson and JET contributors, Comparison of erosion and deposition in JET divertor during the first three ITER-like wall campaigns, Phys. Scr. T171, 2020, 014059 (8pp) https://doi.org/10.1088/1402-4896/ab5c11
[18] Y. Oya, S. Masuzaki, M. Tokitani, M. Nakata, F. Sun, M. Oyaidzu, K. Isobe, N. Asakura, T. Otsuka, A. Widdowson, J. Likonen, M. Rubel and JET Contributors, *Comparison of Hydrogen Isotope Retention in Divertor Tiles of JET with the ITER-Like Following Campaigns in 2011-2012 and 2015-2016*, Fusion Sci. and Technol. 76, 2020, 439-445 https://doi.org/10.1080/15361055.2020.1716455
[19] A. Widdowson, C. F. Ayres, S. Booth, J.P. Coad, A. Hakola, K. Heinola, D. Ivanova, S. Koivuranta, J. Likonen, M. Mayer, M. Stamp, JET-EFDA Contributors, *Comparison of JET main chamber erosion with dust collected in the divertor,* J. Nucl. Mater. 438, 2013, p. S827 – S832 https://doi.org/10.1016/j.jnucmat.2013.01.179
[20] A. Widdowson, E. Alves, C.F. Ayres, A. Baron-Wiechec, S. Brezinsek, N. Catarino, J.P. Coad, K. Heinola, J. Likonen, G.F. Matthews, M. Mayer, M. Rubel and JET-EFDA Contributors, *Material migration patterns and overview of first surface analysis of the JET ITER-like wall*, Phys. Scr. T159, 2014, 014010 (9pp) https://doi.org/10.1088/0031-8949/2014/T159/014010
[21] K. Heinola, C.F. Ayres, A. Baron-Wiechec, J.P. Coad, J. Likonen, G.F. Matthews, A. Widdowson and JET –EFDA Contributors, *Tile profiling analysis of sample from the JET ITER-like wall and carbon wall*, Phys. Scr. T159, 2014, 014013 (5pp) https://doi.org/10.1088/0031-8949/2014/T159/014013
[22] A. Baron-Wiechec, A. Widdowson, E. Alves, C.F. Ayres, N.P. Barradas, S. Brezinsek, J.P. Coad, N. Catarino, K. Heinola, J. Likonen, G.F. Matthews, M. Mayer, P. Petersson, M. Rubel, W. van Renterghem, I. Uytdenhouwen, JET-EFDA contributors, *Global erosion and deposition in JET with the ITER-like wall*, J. Nucl. Mater. 463, 2015, p. 157-161 https://doi.org/10.1016/j.jnucmat.2015.01.038
[23] K. Heinola, A. Widdowson, J. Likonen, E. Alves, A. Baron-Wiechec, N. Barradas, S. Brezinsek, N. Catarino, P. Coad, Koivurant, G.F. Matthews, M. Mayer, P. Petersson, JET-EFDA

Contributors, *Fuel retention in JET ITER-like Wall from post-mortem analysis*, J Nucl. Mater. 463, 2015, p. 961 - 965 https://doi.org/10.1016/j.jnucmat.2014.12.098
[24] K. Heinola, A. Widdowson, J. Likonen, E. Alves, A. Baron-Wiechec, N. Barradas, S. Brezinsek, N. Catarino, P. Coad, S. Koivuranta, S. Krat, G.F. Matthews, M. Mayer, P. Petersson and JET Contributors, *Long-term fuel retention in JET ITER-like wall*, Phys. Scr. T167, 2016, 014075 (7pp) https://doi.org/10.1088/0031-8949/T167/1/014075
[25] A. Widdowson, J.P. Coad, E. Alves, A. Baron-Wiechec, N.P. Barradas, S. Brezinsek, N. Catarino, V. Corregidor, K. Heinola, S. Koivuranta, S. Krat, A. Lahtinen, J. Likonen, G.F. Matthews, M. Mayer, P. Petersson, M. Rubel and JET Contributors, *Overview of fuel inventory in JET with the ITER-like wall*, Nucl. Fusion 57, 2017, 086045 (9pp) https://doi.org/10.1088/1741-4326/aa7475
[26] A. Widdowson, S. Aliferis, E. Alves, L. Avotina, A. Baron-Wiechec, N. Catarino, J.P. Coad, V. Corregidorm K. Heinola, I. Jepu, C. Makepeace and JET Contributors, *Fuel inventory and material migration of JET main chamber plasma facing components compared over three operation periods,* Phys. Scr. 171, 2020, 014051 (8pp) https://doi.org/10.1088/1402-4896/ab5350
[27] M. Rubel, P. Petersson, E. Alves, S. Brezinsek, J.P. Coad, K. Heinola, M. Mayer, A. Widdowson, JET Contributors, *The role and application of ion beam analysis for studies of plasma-facing components in controlled fusion devices*, Nucl. Instr. and Meth. in Phys. Res. B 371, 2016, 4-11 https://doi.org/10.1016/j.nimb.2015.09.077
[28] M. Rubel, P. Petersson, Y. Zhou, J.P. Coad, C. Lungu, I. Jepu, C. Porosnicu, D. Matveev, A. Kirschner, S. Brezinsek, A. Widdowson, E. Alves and JET Contributors, *Fuel inventory and deposition in castellated structures in JET-ILW*, Nucl. Fusion 57, 2017, 066027 (7pp) https://doi.org/10.1088/1741-4326/aa6864
[29] P. Tsavalas, A. Lagoyannis, K. Mergia, M. Rubel, K. Triantou, S. Harissopulos, M. Kokkoris, P. Petersson and JET Contributors, *Be ITER-like wall at the JET tokamak under plasma*, Phys. Scr. T170, 2017, 014049 (8pp) https://doi.org/10.1088/1402-4896/aa8ff4
[30] G.F. Matthews, JET EDFA Contributors, the ASDEX-Upgrade Team, *Plasma operation with an all metal first-wall: Comparison of an ITER-like wall with a carbon wall in JET*, J. Nucl. Mater. 438, 2013, S2-S10 https://doi.org/10.1016/j.jnucmat.2013.01.282
[31] T. Loarer, S. Brezinsek, V. Philipps, J. Bucalossi, D. Douai, H.G. Esser, S. Grunhagen, J. Hobirk, S. Jachmich, E. Joffrin, U. Kruezi, C. Lowry, G. Matthews, R. Smith, E. Tsitrone, S. Vartanian, JET-EFDA Contributors, *Comparison of long term fuel retention in JET between carbon and ITER-Like Wall*, J. Nucl. Matter. 438, 2013, S108-S113 https://doi.org/10.1016/j.jnucmat.2013.01.017
[32] S. Brezinsek, S. Jachmich, M.F. Stamp, A.G. Meigs, J.W. Coenen, K. Krieger, C. Giroud, M. Groth, V. Philipps, S. Grunhagen, R. Smith, G.J. van Rooij, D. Ivanova, G.F. Mathews, JET-EFDA contributors, *Residual carbon content in the initial ITER-Like Wall experiments at JET*, J. Nucl. Matter. 438, 2013, S303-S308 https://doi.org/10.1016/j.jnucmat.2013.01.122
[33] R. A. Anderl, G.R. Longhust, R.J. Pawelko and M.A. Oates, *Implanted Deuterium Retention and Release in Carbon-Coated Beryllium*, Journal of Fusion Energy, Vol. 16, Nos1/2, 1997 10.1023/A:1022569130666
[34] M. I. Guseva, V. M. Gureev, L. S. Danelyan, B. N. Kolbasov, S. N. Korshunov, Yu. V. Sereda, V.G. Stolyarova, V.V. Zatekin, and V.S. Kulikauskas, Effect of Carbon on Accumulation of Deuterium in beryllium Irradiated with Stationary Plasma, Journal of Surface Investigation Vol. 2, No. 2, 2008, pp. 274-276 https://doi.org/10.1134/S1027451008020201
[35] C. Porosnicu, A. Anghel, K. Sugiyama, K. Krieger, J. Roth, C.P. Lungu, *Influence of beryllium carbide formation on deuterium retention and release*, J. Nucl. Mater. 415, 2011, S713-S716 10.1016/j.jnucmat.2010.12.238

[36] M. Mayer, S. Moller, M. Rubel, A. Widdowson, S. Charisopoulos, T. Ahlgren, E. Alves, G. Apostolopoulos, N.P. Barradas, S. Donnelly, S. Fazinic, K. Heinola, O. Kakuee, H. Khodja, A. Kimura, A. Lagoyannis, M. Li, S. Markelj, M. Mudrinic, P. Petersson, I. Portnykh, D. Primetzhofer, P. Reichart, D. Ridikas, T. Silva, S.M. Gonzalez de Vicente and Y.Q. Wang, *Ion beam analysis of fusion plasma-facing materials and components: facilities and research challenges*, Nucl. Fusion 60, 2020, 025001 https://doi.org/10.1088/1741-4326/ab5817
[37] M. Rubel, J. P. Coad, R. A. Pitts, Contributors to the JET-EFDA Workprogramme, *Overview of co-eposition and fuel inventory in castellated divertor structures at JET*, J. Nucl. Mater. 367-370, 2007, 1432-1437 https://doi.org/10.1016/j.jnucmat.2007.04.007
[38] M. Rubel, J. P. Coad, D. Hole, JET-EFDA Contributors, *Overview of long-term fuel inventory and co-deposition in castellated beryllium limiters at JET*, J. Nucl. Mater., 386-388, 2009, 739-732 https://doi.org/10.1016/j.jnucmat.2008.12.287
[39] V. Ricardo, P. Lomas, G.F. Matthews, I. Nunes, V. Thompson, E. Villedieu and JET EFDA Contributors, Design, Manufacture and Initial Operation of the Beryllium Component of the JET ITER-Like Wall, Fusion Eng. and Design, 88 2013, 585-589 https://doi.org/10.1016/j.fusengdes.2013.01.084
[40] C. P. Lungu, I. Mustata, V. Zaroschi, A.M. Lungu, A. Aughel, P. Chiru, M. Rubel, P. Coad, G.F. Matthews and JET-EFDA contributors, *Beryllium coatings on metals for marker tiles at JET: development of process and characterization of layer*, Phys. Scr. T128, 2007, 157-161 https://doi.org/10.1088/0031-8949/2007/T128/030
[41] http://www.microbeams.co.uk/index.html
[42] M. Bogovac, I. Bogdanovic, S. Fazinic, M. Jaksic, L. Kukec, W. Wilhelm, *Data acquisition and scan control system for nuclear microprobe and other mulitparameter experiments,* Nucl. Instr. and Meth. in Phys. Res. B 89, 1994, 219-222 https://doi.org/10.1016/0168-583X(94)95176-4
[43] S. Fazinić, T. Tadic, M. Vuksic, M. Rubel, P. Petersson, E. Fortuna-Zalesna and A. Widdowson, Ion Microbeam Analyses of Dust Particles and Codposits form JET with the ITER-Like Wall, *Anal. Chem.* 2018, 90, 9, 5744–5752 https://doi.org/10.1021/acs.analchem.8b00073
[44] M. Mayer, *SIMNRA, a simulation program for the analysis of NRA, RBS and ERDA, AIP Conf. Proc.*, 475, 1999, 541–544 https://doi.org/10.1063/1.59188
[45] V. Kh. Alimov, M. Mayer, J. Roth, *Differential cross-section of the D(3He,p)4He nuclear reaction and depth profiling of deuterium up to large depths*, Nucl. Instr. and Meth. in Phys. Res. B, 234, 2005, 169-175 https://doi.org/10.1016/j.nimb.2005.01.009
[46] N. P. Barradas, N. Catarino, R. Mateus, S. Magalhaes, E. Alves, Z. Siketic, I. Bogdanovic Radovic, *Determination of the 9 Be(3He,pi)11B (i=0,1,2,3) cross section at 135 degrees in the energy range 1-2.5 MeV*, Nucl. Instr. and Meth. in Phys. Res. B 346, 2015, 21-25 https://doi.org/10.1016/j.nimb.2015.01.037
[47] A. F. Gurbich, *SigmaCalc recent development and present status of the evaluated cross-sections for IBA*, Nucl. Instr. and Meth. in Phys. Res B, 271, 2016, 27-32 https://doi.org/10.1016/j.nimb.2015.09.035
[48] P. Tsavalas, A. Lagoyannis, K. Mergia, E. Ntemou, C.P. Lungu, *Differential cross sections of the deuteron reactions on beryllium at energies and angles suitable for nuclear reaction analysis*, Nucl. Instr. and Meth. in Phys. Res. B, 479, 2020, 205-210 https://doi.org/10.1016/j.nimb.2020.07.002